

# X. MANGANESE NODULE OCCURRENCE AND BENTHONIC ACTIVITIES OBSERVED FROM DEEP SEA PHOTOGRAPHS IN THE GH78-1 AREA

*Yasumasa Kinoshita and Tomoyuki Moritani*

## Introduction

Deep sea photographs in the GH78-1 cruise were obtained by two methods, namely a one-shot 16 mm camera attached to the freefall (boomerang) type photo grab and an independent 35 mm deep sea camera (Table X-1).

The one-shot 16 mm camera system is the product of the Preussag Co., West Germany, with an installed 16 mm Minolta camera. The camera system is attached to the freefall sampler, and works to take a picture of sea bottom by releasing of shutter just before the sampler hits the bottom at about 1.2 m distance above the bottom.

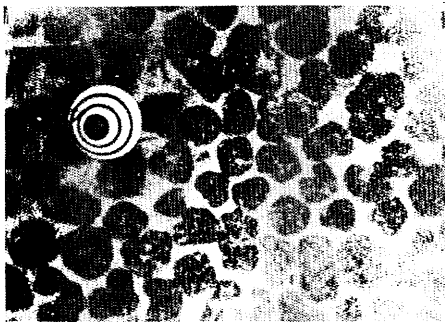
Near each sampling station by wire-lined grab and other samplers, two sets of the freefall sampler were used simultaneously, and 72 photographs were obtained as shown in Fig. X-1 (1-15).

The 35 mm deep sea camera system is the product of the Benthos Inc., U.S.A., consisting of Edgerton 35 mm deep sea camera (Model 382). At St. 1068 (C-13) and St. 1076 (C-14), a range of the bottom was continuously photographed in 6 sec. intervals using a timer.

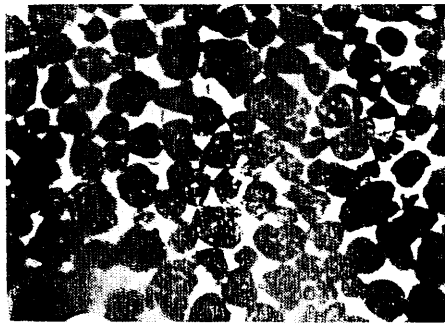
As a result of the operation of the system, 210 frames of sea bottom pictures were obtained at St. 1068 (C-13) in 80 minutes drifting, and 458 frames of that at St. 1076 (C-14) in 85 minutes drifting.

Table X-1 Photographing condition

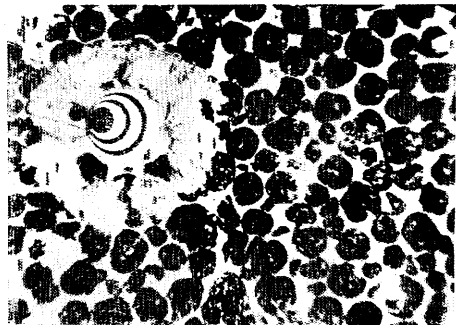
35 mm deep sea camera		
Station no.	1068 (C-13)	1076 (C-14)
Distance	2 m	2 m
F. stop	5.6	5.6
Film	KODAK PLUS-Pan film black-and-white 100 ft ASA 125	KODAK PLUS-Pan film black-and-white 100 ft ASA 125
Photographing interval	6 sec	6 sec
Photographing time	80 min	85 min
16 mm camera of freefall photo grab		
Distance	1.2 m	
F. stop	5.6-8	
Film	Minolta 16 black-and-white	



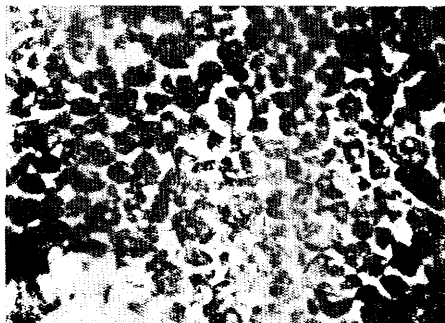
ST.1036 FG73-1 10cm  
5174m , 32.0kg/m<sup>2</sup>



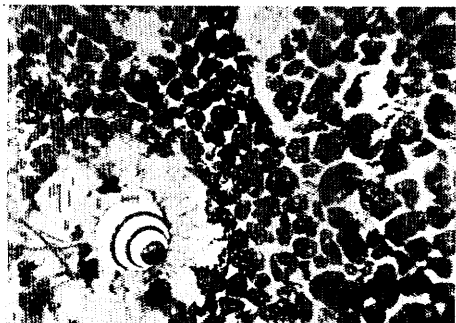
ST.1037 FG74-1  
5020m , 20.8kg/m<sup>2</sup>



ST.1037 FG74-2 10cm  
5040m , 26.0kg/m<sup>2</sup>



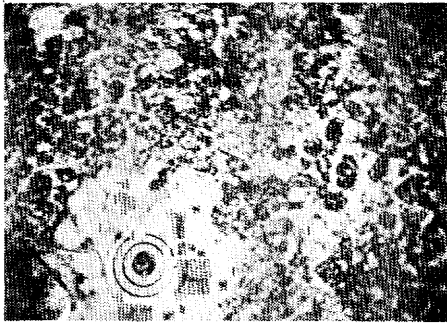
ST.1038 FG75-1  
5952m , 13.0kg/m<sup>2</sup>



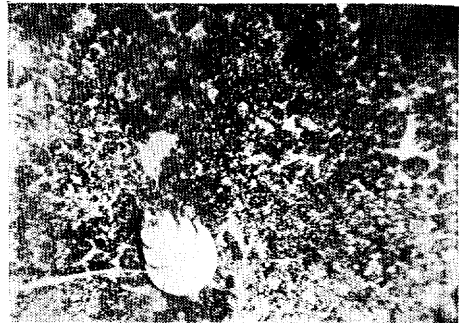
ST.1038 FG75-2 10cm  
5952m , 6.9kg/m<sup>2</sup>

(1)

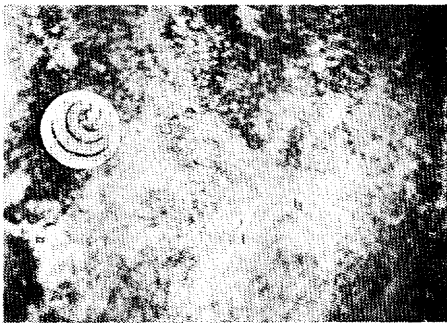
Fig. X-1 (1-15) Sea bottom photographs by the one-shot 16 mm camera of free-fall photo grab sampler at each station. The data accompanying each figure indicate station number (St.), observation number (FG=freefall grab), water depth, manganese nodule abundance (in kg/m<sup>2</sup>), and scale (10 cm) respectively.



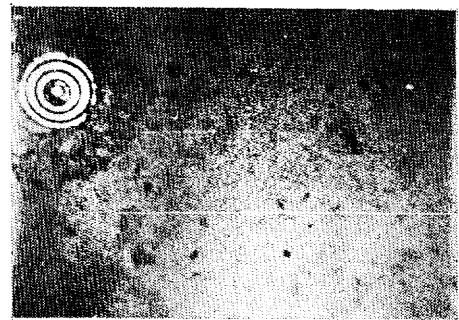
ST.1039 FG76-1 10cm  
5020m , 2.2kg/m<sup>2</sup>



ST.1039 FG76-2 10cm  
5030m , 0.0kg/m<sup>2</sup>

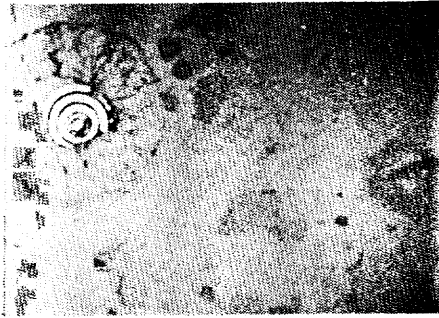


ST.1040 FG77-1 10cm  
5256m



ST.1041 FG78-2 10cm  
5680m , trace

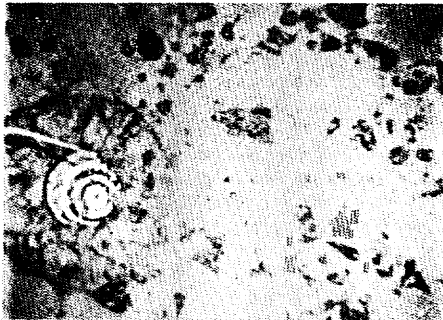
(2)



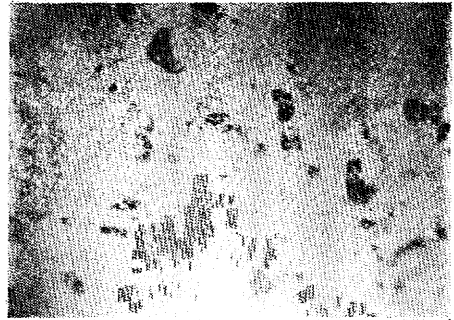
ST.1042 FG79-1  
5813m , trace 10cm



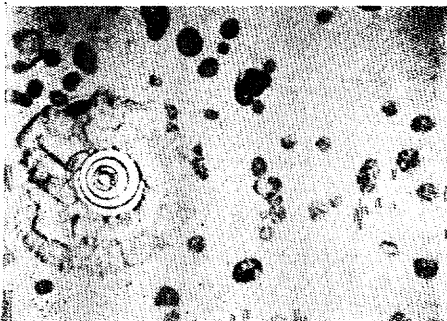
ST.1042 FG79-2  
5813m , trace



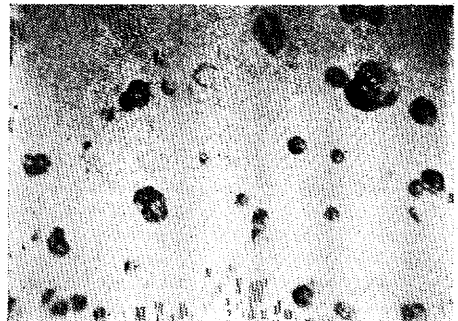
ST.1043 FG80-1  
5608m , trace 10cm



ST.1043 FG80-2  
5618m , trace

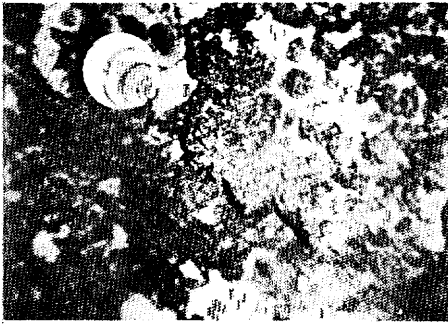


ST.1044 FG81-1  
5360m ,  $2.6\text{kg/m}^2$  10cm



ST.1044 FG81-2  
5370m ,  $1.8\text{kg/m}^2$

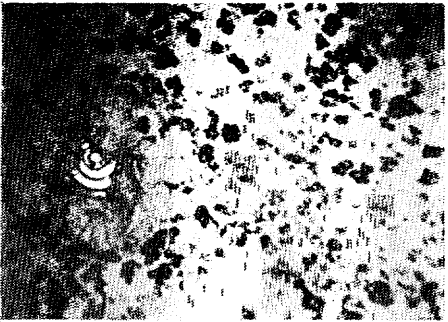
(3)



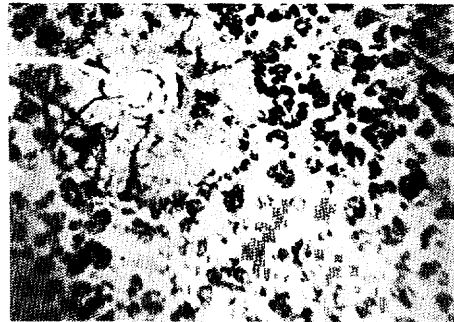
ST.1045 FG82-1 10cm  
5246m , trace



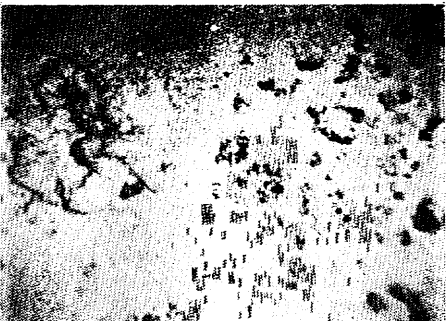
ST.1045 FG82-2 10cm  
5246m ,



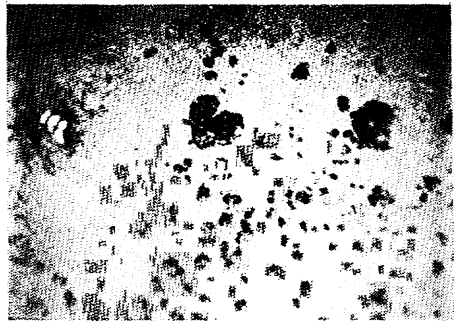
ST.1046 FG83-1 10cm  
5463m , 6.0kg/m<sup>2</sup>



ST.1046 FG83-2 10cm  
5433m , 7.7kg/m<sup>2</sup>

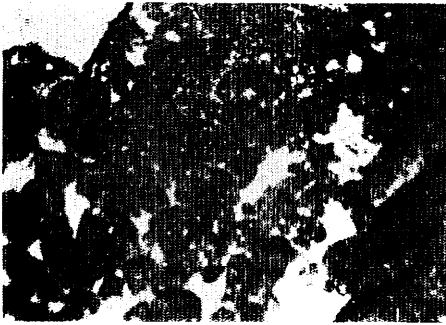


ST.1047 FG84-1  
5660m , 2.6kg/m<sup>2</sup>



ST.1047 FG84-2  
5649m , 4.3kg/m<sup>2</sup>

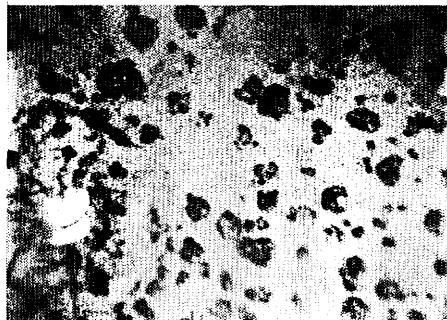
(4)



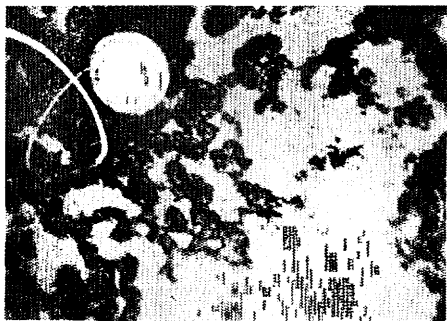
ST.1048 FG85-1  
5153m , trace



ST.1048 FG85-2  
5153m , 6.9kg/m<sup>2</sup> 10cm

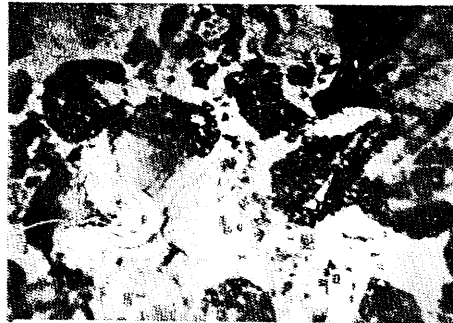


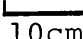
ST.1049 FG86-2  
5973m , 9.5kg/m<sup>2</sup> 10cm

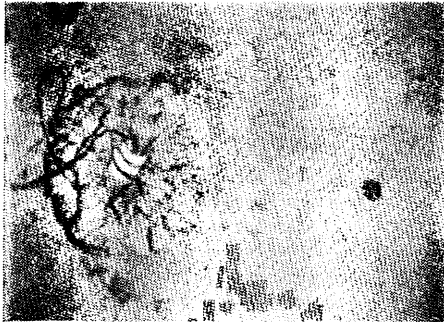


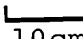
ST.1050 FG87-2  
5618m , 10cm

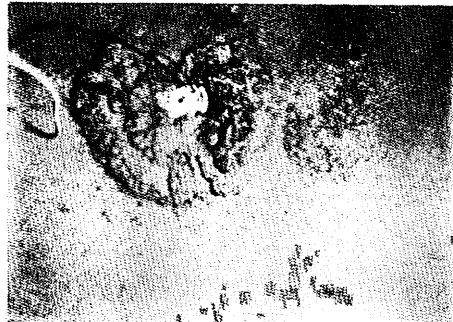
(5)

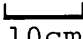


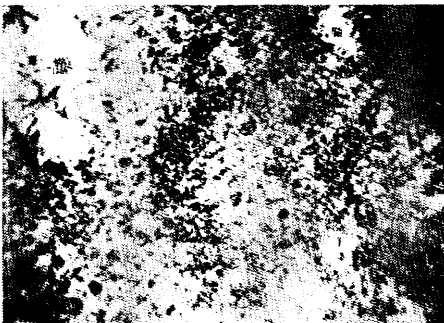
ST.1051 FG88-2  
5245m ,  10cm



ST.1052 FG89-1  
5931m , 0.9kg/m<sup>2</sup>  10cm

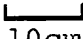


ST.1052 FG89-2  
5931m , trace  10cm

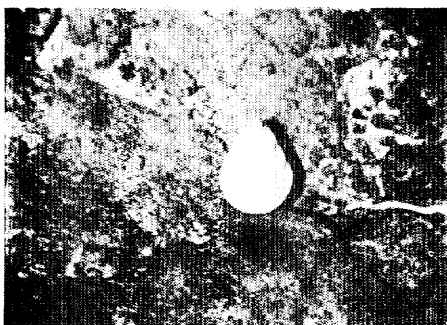


ST.1053 FG90-1  
4782m , 2.6kg/m<sup>2</sup>

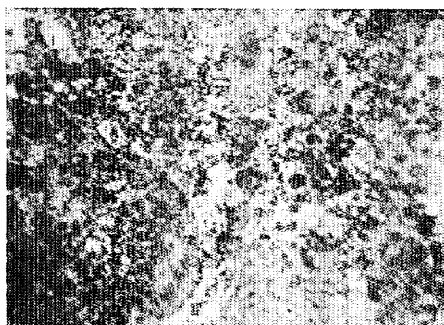


ST.1053 FG90-2  
4813m , trace  10cm

(6)



ST.1054 FG91-1  
4875m , ┌───┐  
10cm



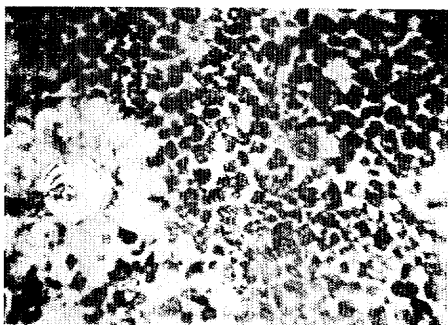
ST.1054 FG91-2  
4762m , 4.6kg/m<sup>2</sup>



ST.1055 FG94-1  
5952m , 0.8kg/m<sup>2</sup>



ST.1055 FG94-2  
5952m , trace ┌───┐  
10cm



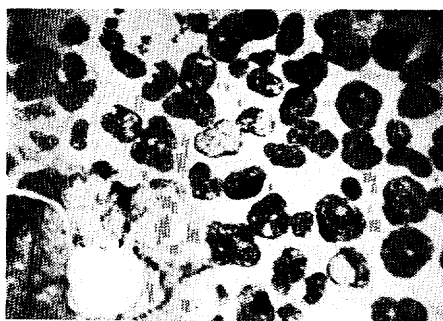
ST.1056 FG95-1  
5952m , 10.0kg/m<sup>2</sup> ┌───┐  
10cm



ST.1056 FG95-2  
5930m , 15.4kg/m<sup>2</sup> ┌───┐  
10cm

(7)

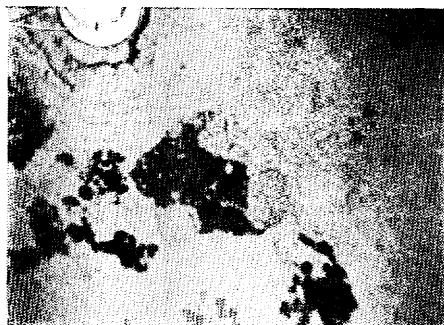




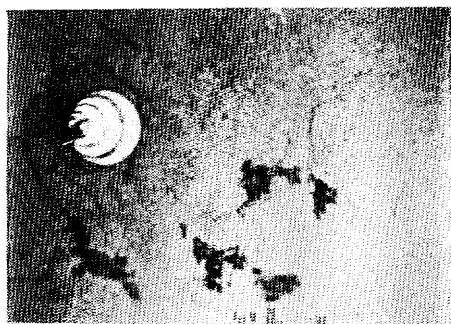
ST.1057 FG96-2  
5952m , 19.0kg/m<sup>2</sup> 10cm



ST.1058 FG97-1  
6150m , 0.0kg/m<sup>2</sup> 10cm

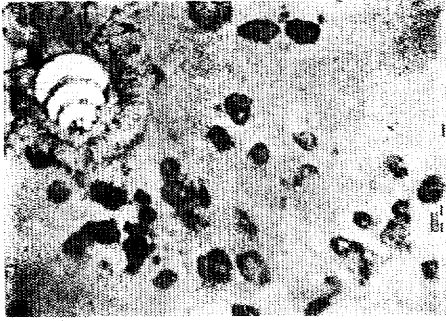


ST.1058 FG97-2  
6150m , 0.0kg/m<sup>2</sup> 10cm

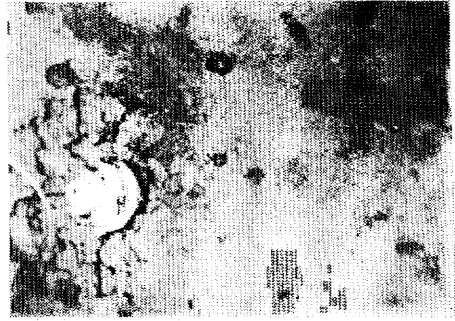


ST.1059 FG98-1  
6056m , 10cm

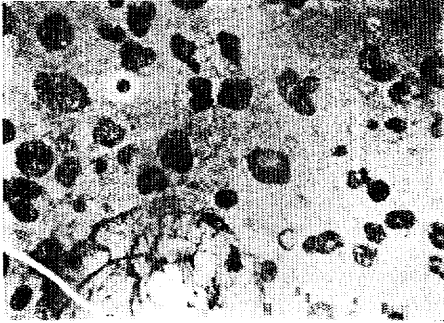
(8)



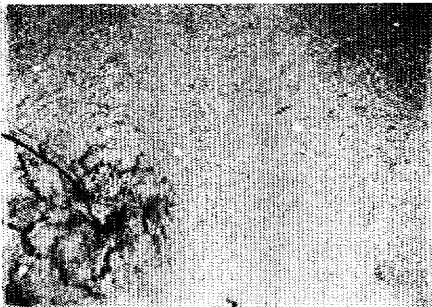
ST.1060 FG92-1  
5700m , 2.2kg/m<sup>2</sup> 10cm



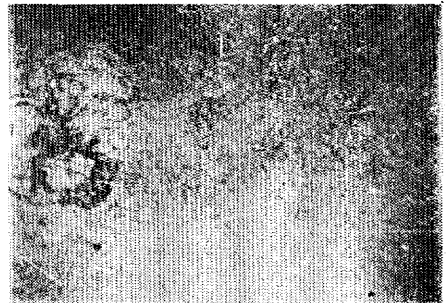
ST.1060 FG92-2  
5710m , 4.3kg/m<sup>2</sup> 10cm



ST.1061 FG93-1  
5639m , 6.1kg/m<sup>2</sup> 10cm

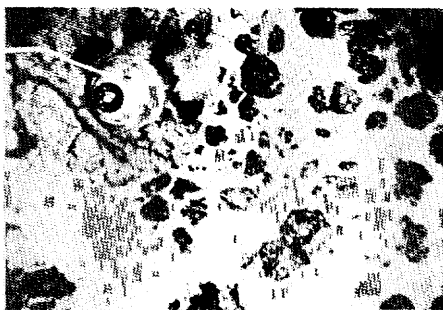


ST.1063 FG99-1  
5433m , 0.0kg/m<sup>2</sup>

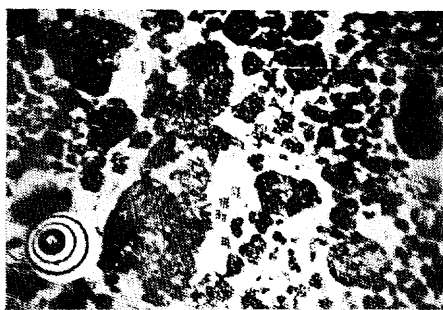


ST.1063 FG99-2  
5433m , 0.0kg/m<sup>2</sup>

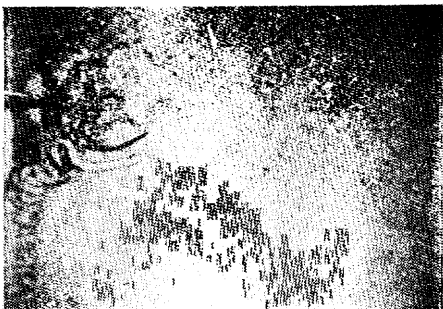
(9)



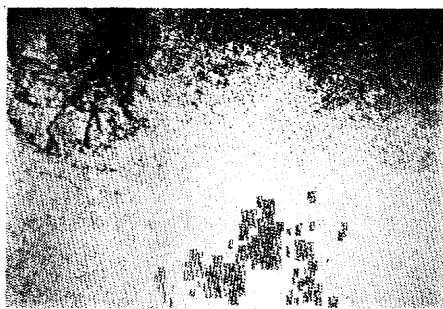
ST.1064 FG100-1  
5245m , 1.7kg/m<sup>2</sup> 10cm



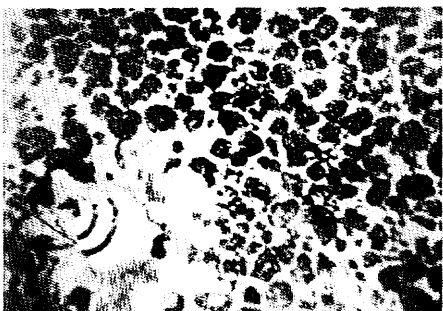
ST.1064 FG100-2  
5328m , 33.7kg/m<sup>2</sup> 10cm



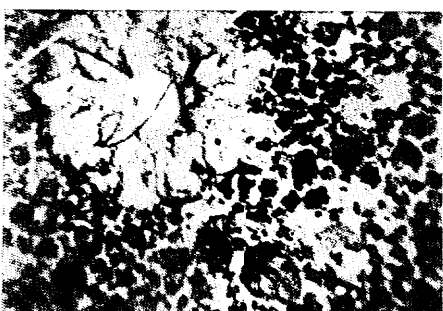
ST.1065 FG101-1  
6159m , trace



ST.1065 FG101-2  
6159m , trace

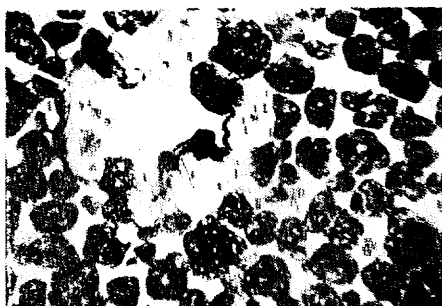


ST.1066 FG102-1  
6263m , 17.3kg/m<sup>2</sup> 10cm

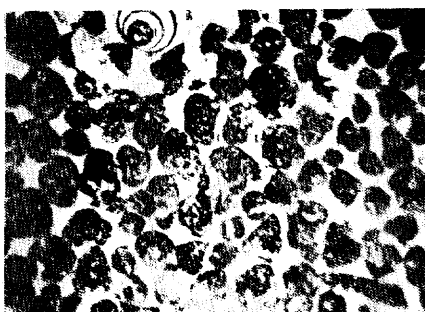


ST.1066 FG102-2  
6263m , 15.5kg/m<sup>2</sup>

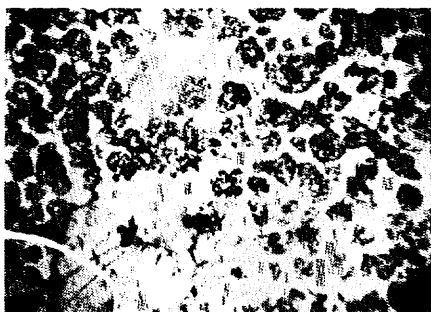
(10)



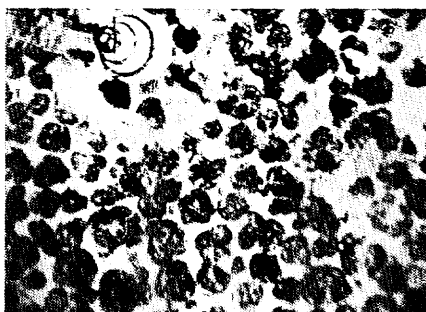
ST.1067 FG103-1  
5370m , 28.5kg/m<sup>2</sup> 10cm



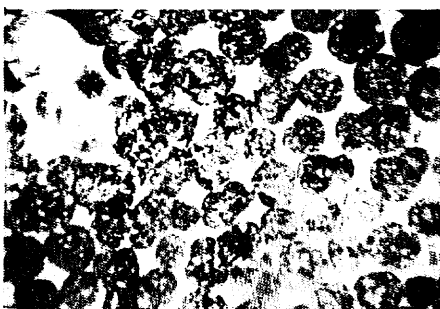
ST.1067 FG103-2  
5340m , 33.7kg/m<sup>2</sup> 10cm



ST.1068 FG104-1  
5433m , 17.7kg/m<sup>2</sup> 10cm



ST.1068 FG104-2  
5423m , 32.9kg/m<sup>2</sup> 10cm



ST.1069 FG105-1  
5464m , 38.1kg/m<sup>2</sup> 10cm

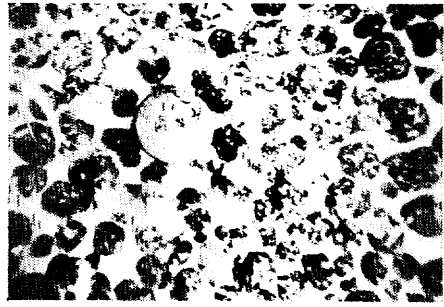


ST.1069 FG105-2  
5433m , 26.8kg/m<sup>2</sup> 10cm

(11)



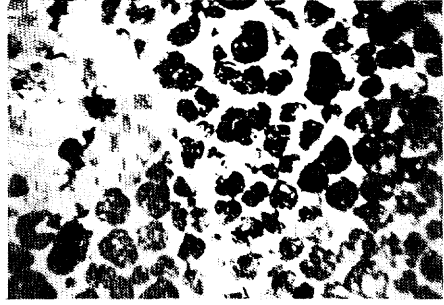
ST.1070 FG106-1  
4968m , 16.4kg/m<sup>2</sup> 10cm



ST.1070 FG106-2  
4948m , 5.2kg/m<sup>2</sup> 10cm



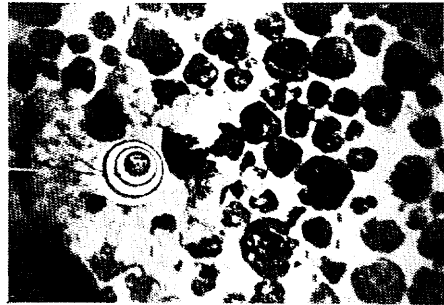
ST.1071 FG107-1  
4919m , 10cm



ST.1071 FG107-2  
4989m , 20.7kg/m<sup>2</sup> 10cm

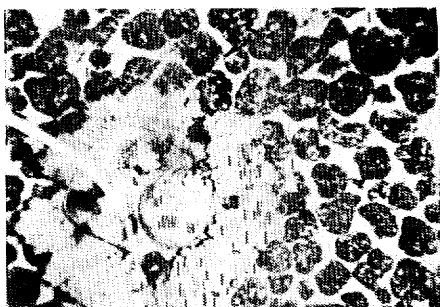


ST.1072 FG108-1  
5754m , 38.1kg/m<sup>2</sup> 10cm

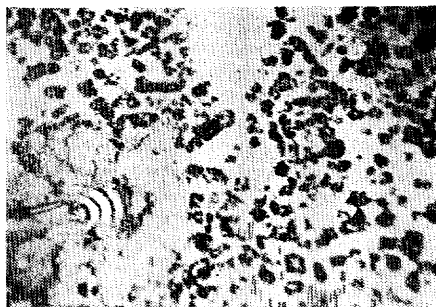


ST.1072 FG108-2  
5774m , 34.6kg/m<sup>2</sup> 10cm

(12)



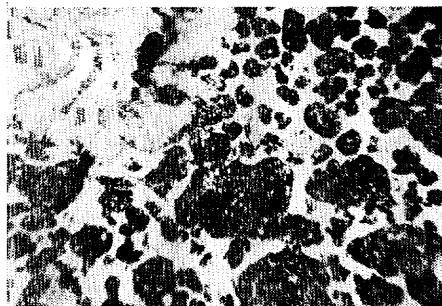
ST.1073 FG109-1  
5164m , 26.8kg/m<sup>2</sup> 10cm



ST.1073 FG109-2  
5287m , 12.1kg/m<sup>2</sup> 10cm



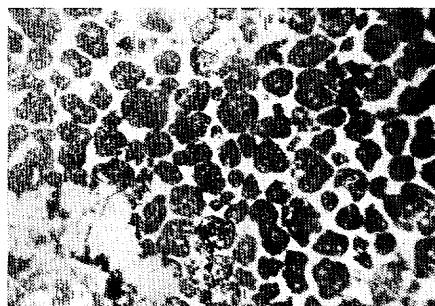
ST.1073 FG109-3  
5329m , 0.0kg/m<sup>2</sup>



ST.1073 FG109-4  
5464m , 32.0kg/m<sup>2</sup>



ST.1074 FG110-1  
5235m , 25.9kg/m<sup>2</sup> 10cm

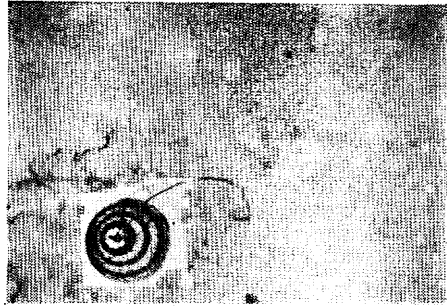


ST.1074 FG110-2  
5225m , 24.2kg/m<sup>2</sup>

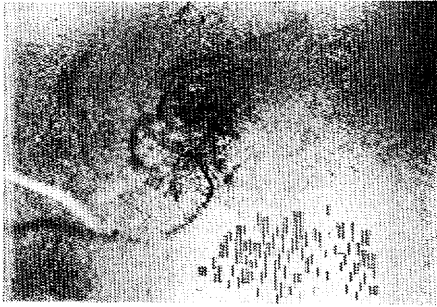
(13)



ST.1075 FG111-1  
3825m , 0.0kg/m<sup>2</sup> 10cm



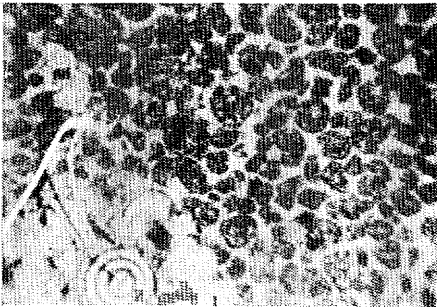
ST.1075 FG111-2  
3916m , 0.0kg/m<sup>2</sup> 10cm



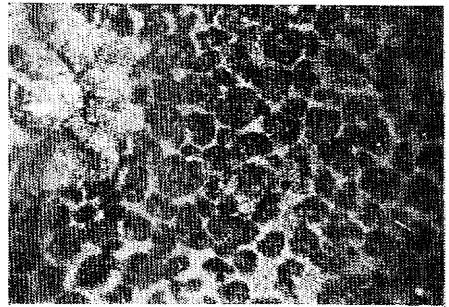
ST.1076 FG112-1  
5454m , 0.35kg/m<sup>2</sup>



ST.1076 FG112-2  
5464m , 2.9kg/m<sup>2</sup>

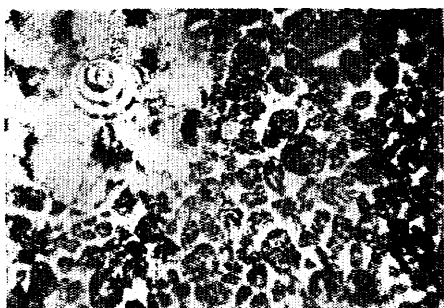



ST.1038-A FG113-1  
6140m , 18.2kg/m<sup>2</sup> 10cm




ST.1038-A FG113-2  
6160m , 20.7kg/m<sup>2</sup> 10cm

(14)



ST.1039-A FG114-1   
5225m , 15.1kg/m<sup>2</sup> 10cm



ST.1039-A FG114-2   
5215m , trace 10cm

(15)

Some typical pictures of them are shown in Figs. X-2-4. The drifting track or speed and direction of the camera are assumed from a series of obtained pictures. At St. 1068 (C-13), the ship was drifting at first towards south with velocity of about 0.1 kt for 23 minutes and then towards northeast with velocity of about 0.2 kt. At St. 1076 (C-14), the motion was at first towards south with velocity of 0.2 kt for 35 minutes, and then towards northwest in about 0.2 kt. Accordingly at St. 1076 (C-14), a span of about 520 m distance of the sea bottom was photographed almost continuously.

Some results of observation on cover ratio and grain size of manganese nodules, and benthonic activities from the obtained pictures are mentioned in the followings.

#### Cover ratio of manganese nodules

Cover ratio of manganese nodules was measured on the photographs using a color index chart. From the results, distribution map of cover ratio was made as Fig. X-5. Two areas of remarkable high cover ratio are recognized both in the southwestern part of the survey area and in the area near Sts. 1053 and 1057, around 10°-11°N. The latter is the western extension part of the high cover ratio zone in the GH77-1 survey area.

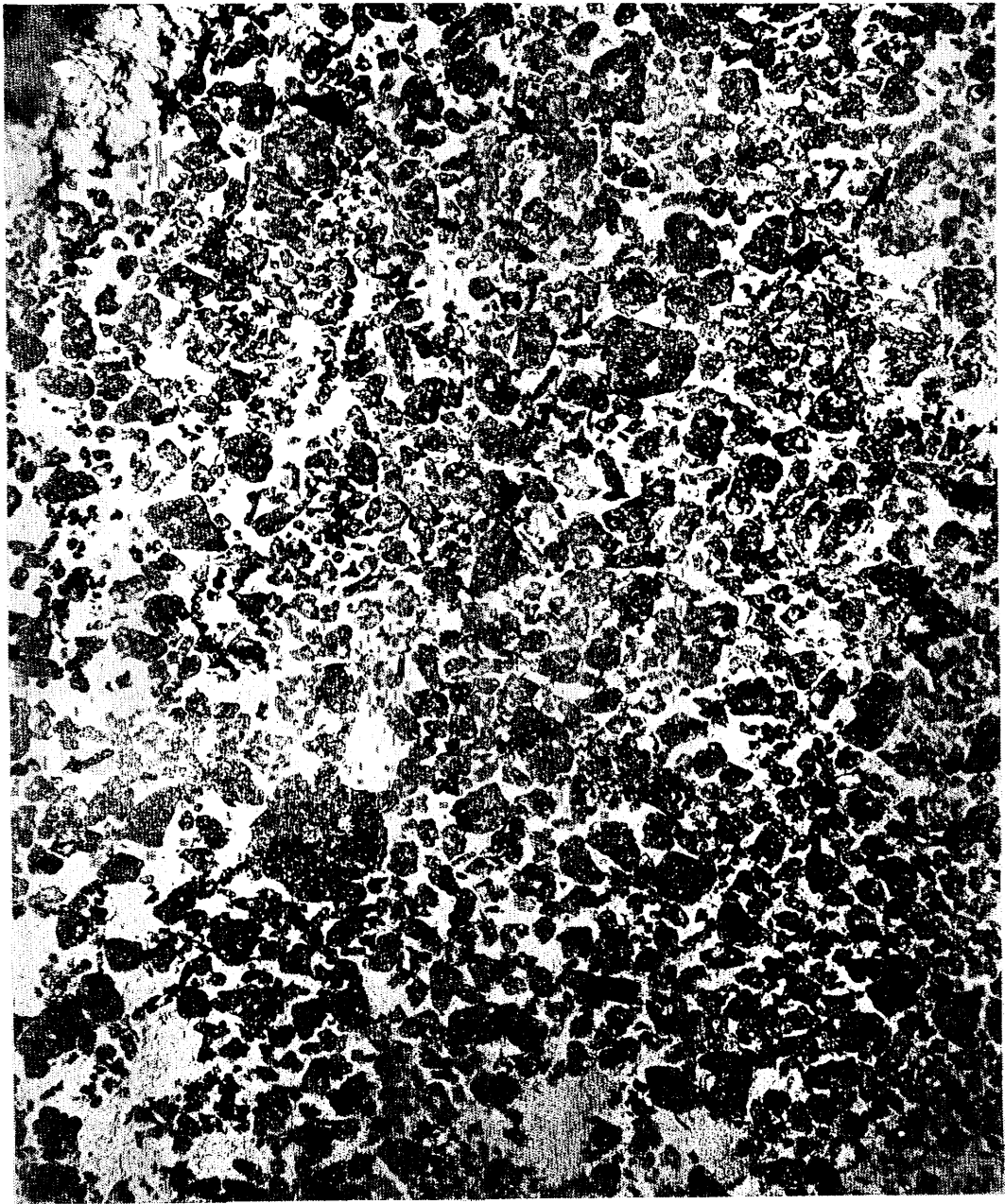
On the other hand, the southwestern high cover ratio area is the mountainous region of rather shallower depth of 5,000-5,500 m as compared with other areas. Although the photographs of St. 1040 (5,256 m), St. 1053 (4,782 m and 4,813 m) and St. 1054 (4,875 m and 4,762 m) show high cover ratio, this is mostly due to rock fragments, and manganese nodules are not abundant judging from the sampling results.

#### Grain size of manganese nodules

On the photographs apparent grain size of manganese nodules was observed, and the median diameter was obtained for each station.

As shown in the distribution map of the median diameter (Fig. X-6), larger median diameter areas coincide with the higher cover ratio areas of the southwestern part and of that around 10°-11°N (St. 1056 and St. 1057). Especially at St. 1036 larger grain size of 4-6 cm order is predominant. Generally speak-

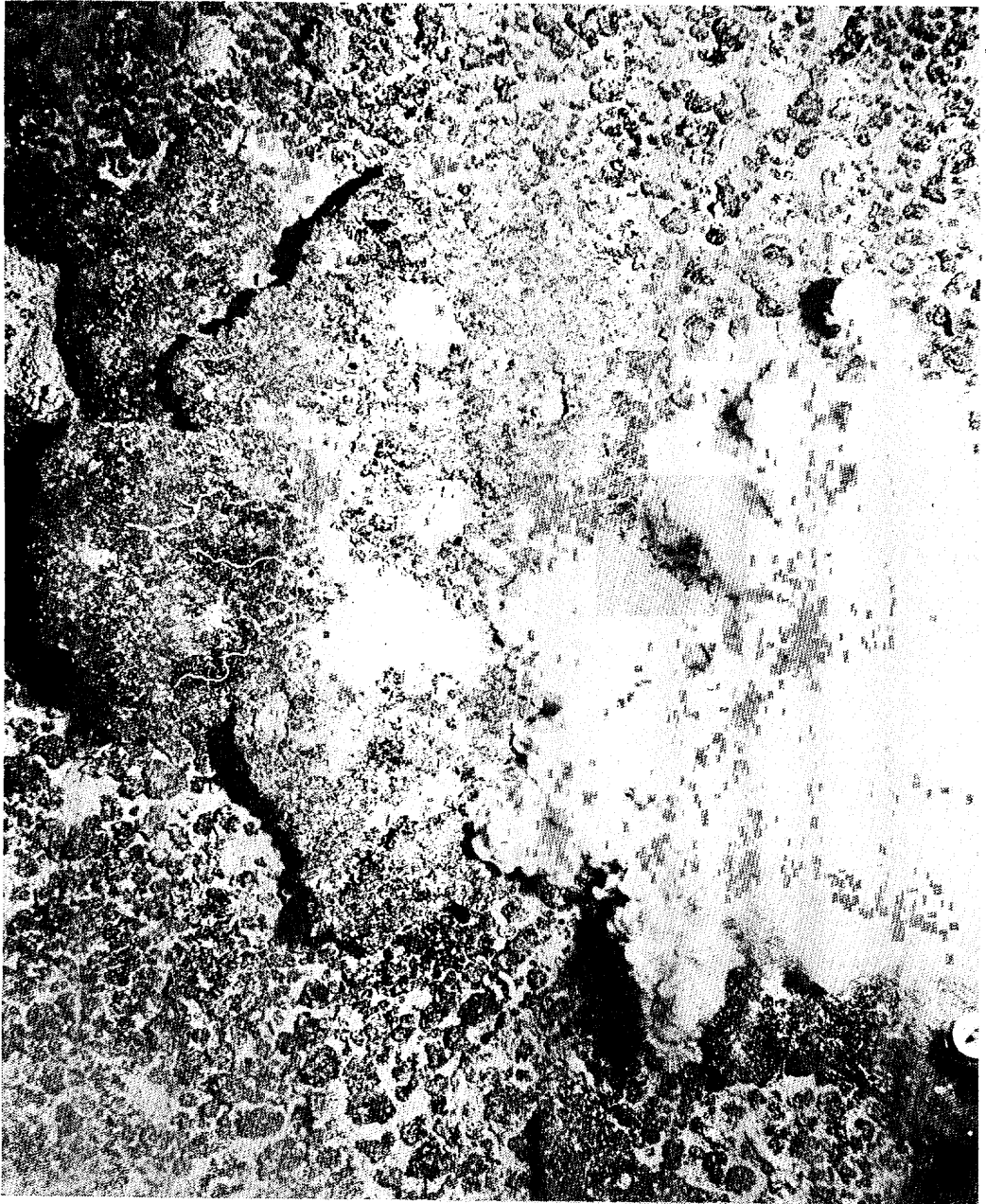




ST.1068 C-13 5443m-5448m

┌───┐  
10cm

Fig. X-2 Sea bottom photograph by 35 mm deep sea camera at St. 1068. The accompany data show observation No. (C-), water depth and scale.



ST.1068 C-13 5443m-5448m

10cm

Fig. X-3 Sea bottom photograph by 35 mm deep sea camera at St. 1068.



ST.1076 C-14 5454m-5464m

┌  
10cm

Fig. X-4 Sea bottom photograph by 35 mm deep sea camera at St. 1076.

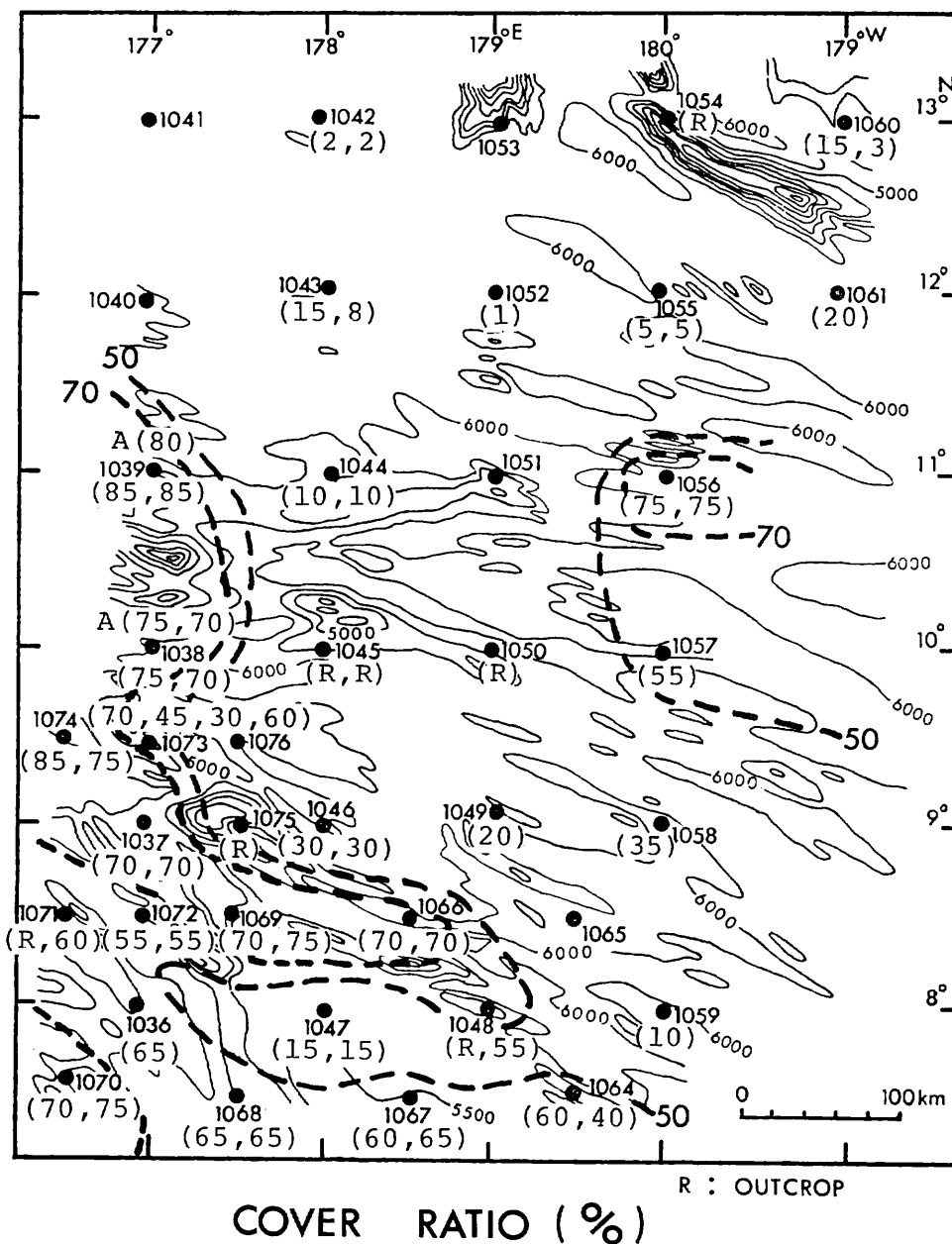
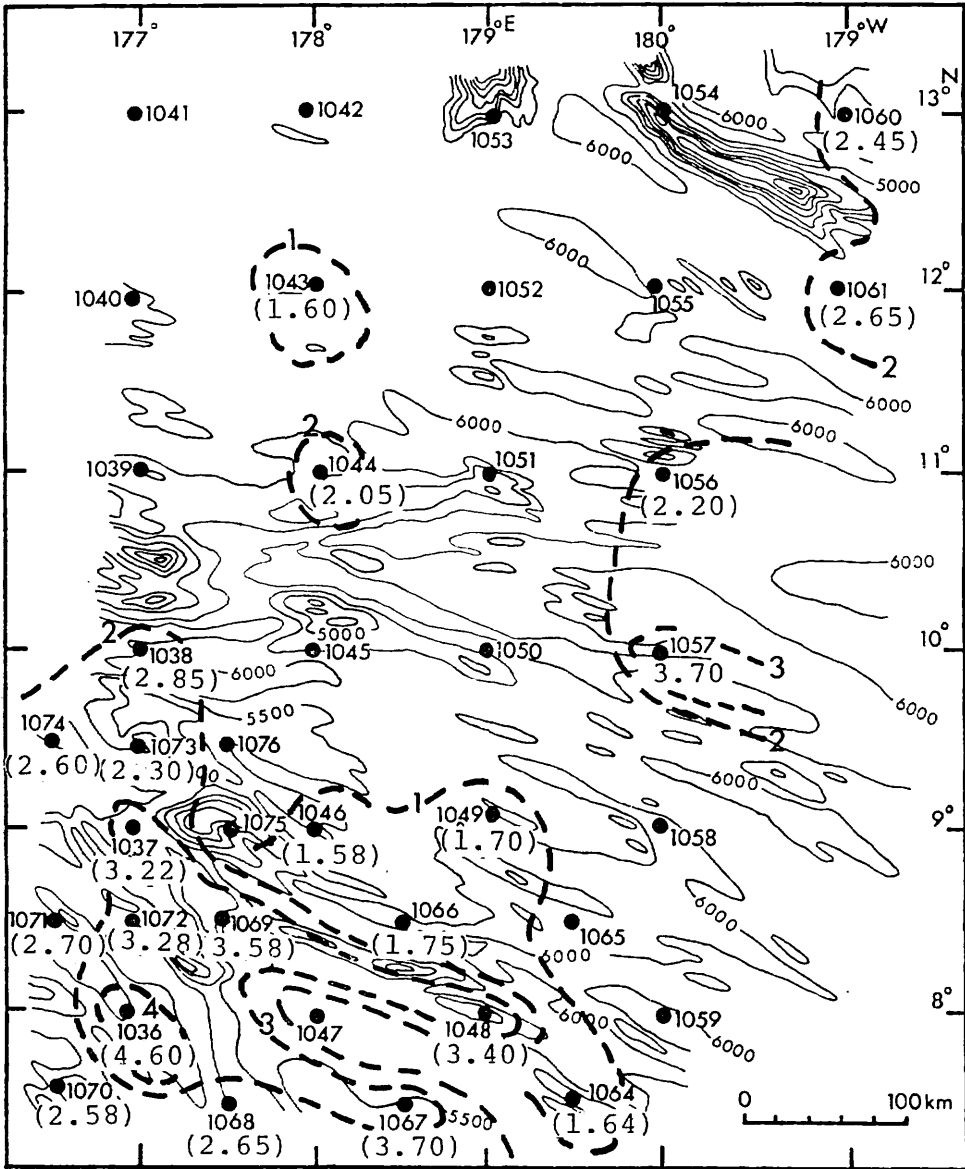


Fig. X-5 Cover ratio of manganese nodules (in %).



## MEDIAN DIAMETER (cm)

Fig. X-6 Median diameter of manganese nodules (in cm).

ing, there is normal correlation between grain size and cover ratio. However, some show higher cover ratio with smaller grain size.

An example of local variation of grain size was indicated in the results of the continuous photographing of the bottom by the 35 mm deep sea camera at St. 1068 (C-13). A span of about 410 m distance of the bottom was photographed into 210 frames of pictures. Among them three typical pictures are shown in Fig. X-7. Here although the cover ratio is almost invariable, the grain size shows a gradual decrease from larger one with angular form at the beginning point of the operation towards northwest. In detail, during 63 m moved distance from the beginning point southward to Frame No. 55, the grain size did not vary, but then during 348 m moved distance diameter of manganese nodules decreased continuously as 2.50 cm at Frame No. 22, 2.20 cm at Frame No. 83, and 1.80 cm at Frame No. 200.

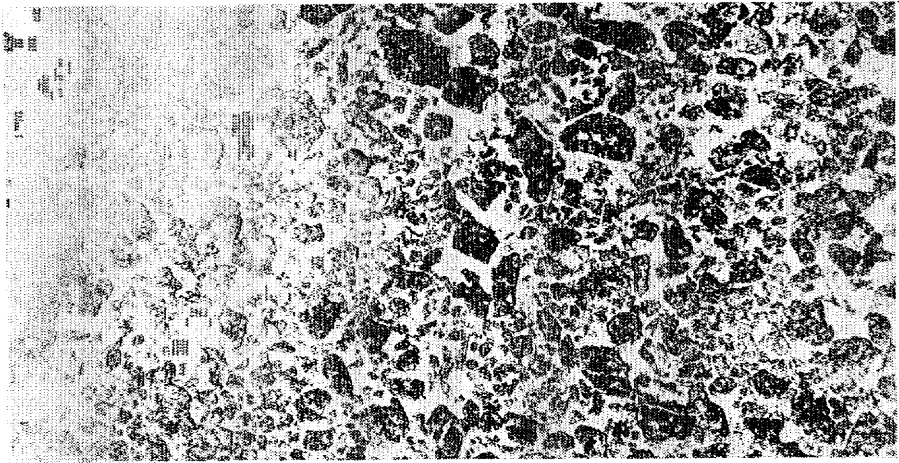
The water depth was 5,443 m at the beginning point and 5,448 m at the end point of photographing operation, although the detailed change of water depth between the two points was not ascertained due to the noise from pinger use in photographing operation against PDR record. A rock predominant zone was recognized between Frame No. 86 to No. 126, but the presence of rocks themselves does not affect the general tendency of cover ratio and grain size changes.

#### **Relation of cover ratio and grain size of manganese nodules to water depth**

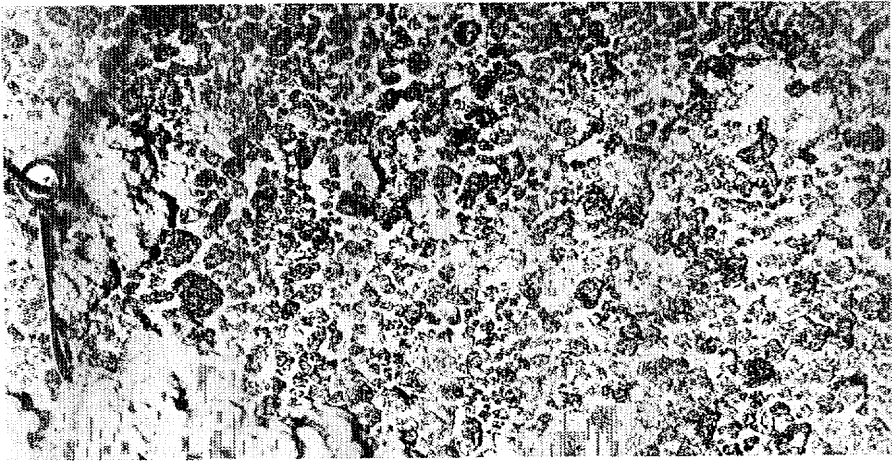
Although for clarifying this relation, we have not detailed data based on a systematic study of nodule distribution in relation to the geographical or topographical conditions, the cover ratio and grain size data of GH77-1 and GH78-1 areas were tentatively plotted against water depth to know a general tendency (Fig. X-8). The result seems to suggest some tendency, namely that nodules are distributed concentrating at least in three water depth zones with a 200 m–300 m range, and that both cover ratio and grain size decrease gradually with increase of water depth in each zone. For example, in the cover ratio, the upper zone shows a decrease from higher part around 5,000 m–5,200 m to lower part around 5,300 m–5,400 m; the middle zone from higher part around 5,400 m–5,600 m to lower part around 5,600 m–5,700 m; and the lower zone from higher part around 5,700 m–6,000 m to 5,900 m–6,100 m. Also the lowest zone may exist with higher ratio part around 5,900 m–6,200 m.

In the grain size or median diameter of nodules, although the upper zone corresponding to that in the cover ratio is not obvious, other corresponding zones have each peak respectively at 5,400 m depth in the middle zone, at 5,800 m in the lower zone and at 6,100 m in the lowest zone, and along each zone also the grain size decreases in accordance with the increase in water depth.

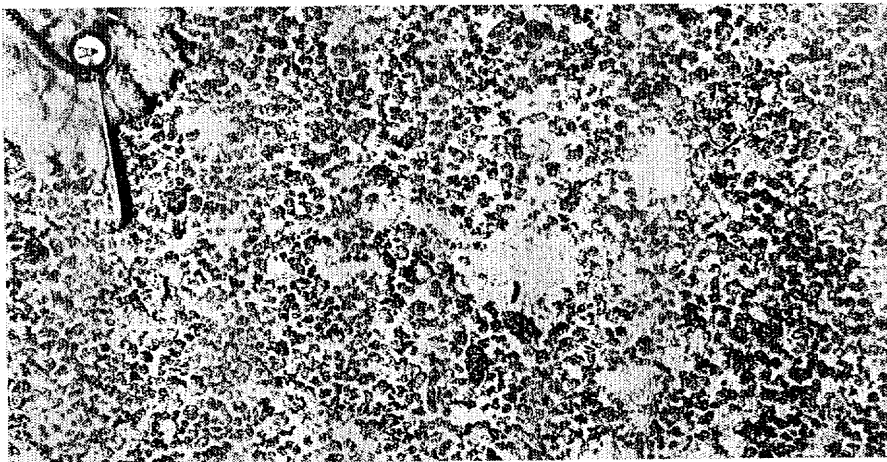
The above-mentioned tendency may suggest the zonal distribution of manganese nodules, showing decrease of both cover ratio and grain size in accordance with increase water depth in each zone. This is, however, a preliminary result, and should be proved by the detailed sampling of nodules in a particular area in relation to the topographical or water depth change.



FRAME NO. 22



FRAME NO. 83



FRAME NO. 200

ST. 1068 C-13 5443m-5448m

10cm

Fig. X-7 Sea bottom photographs by 35 mm deep sea camera at St. 1068, showing local variation of grain size of manganese nodules.

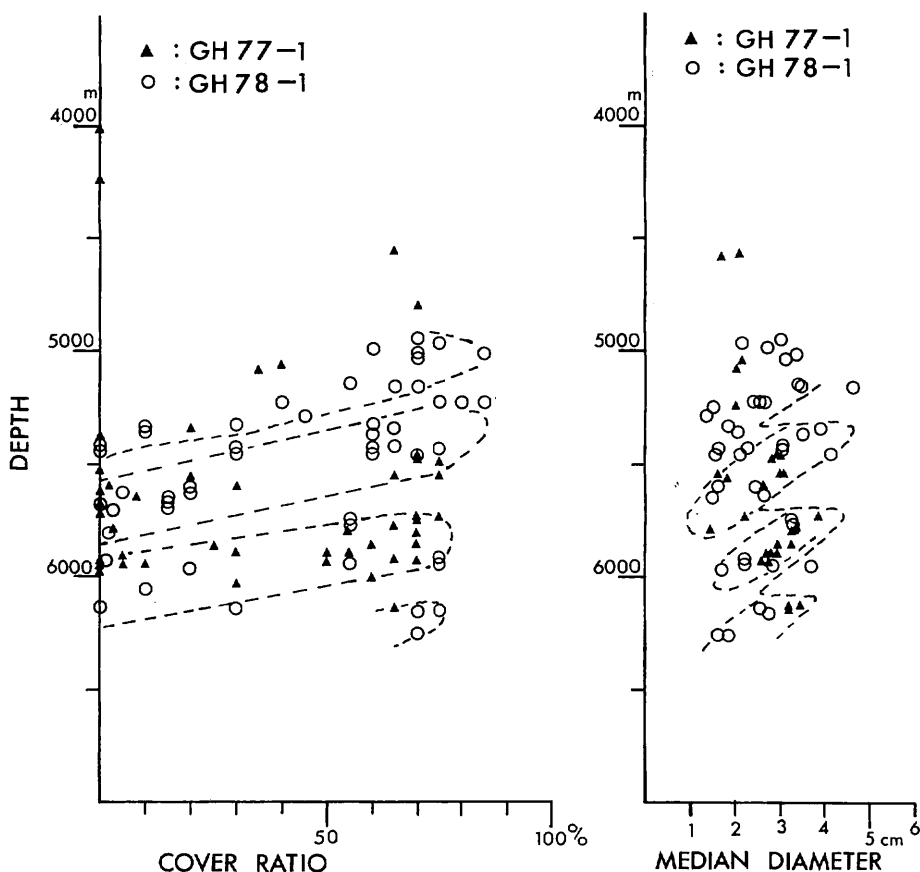


Fig. X-8 Relation of cover ratio and median diameter of manganese nodules to water depth.

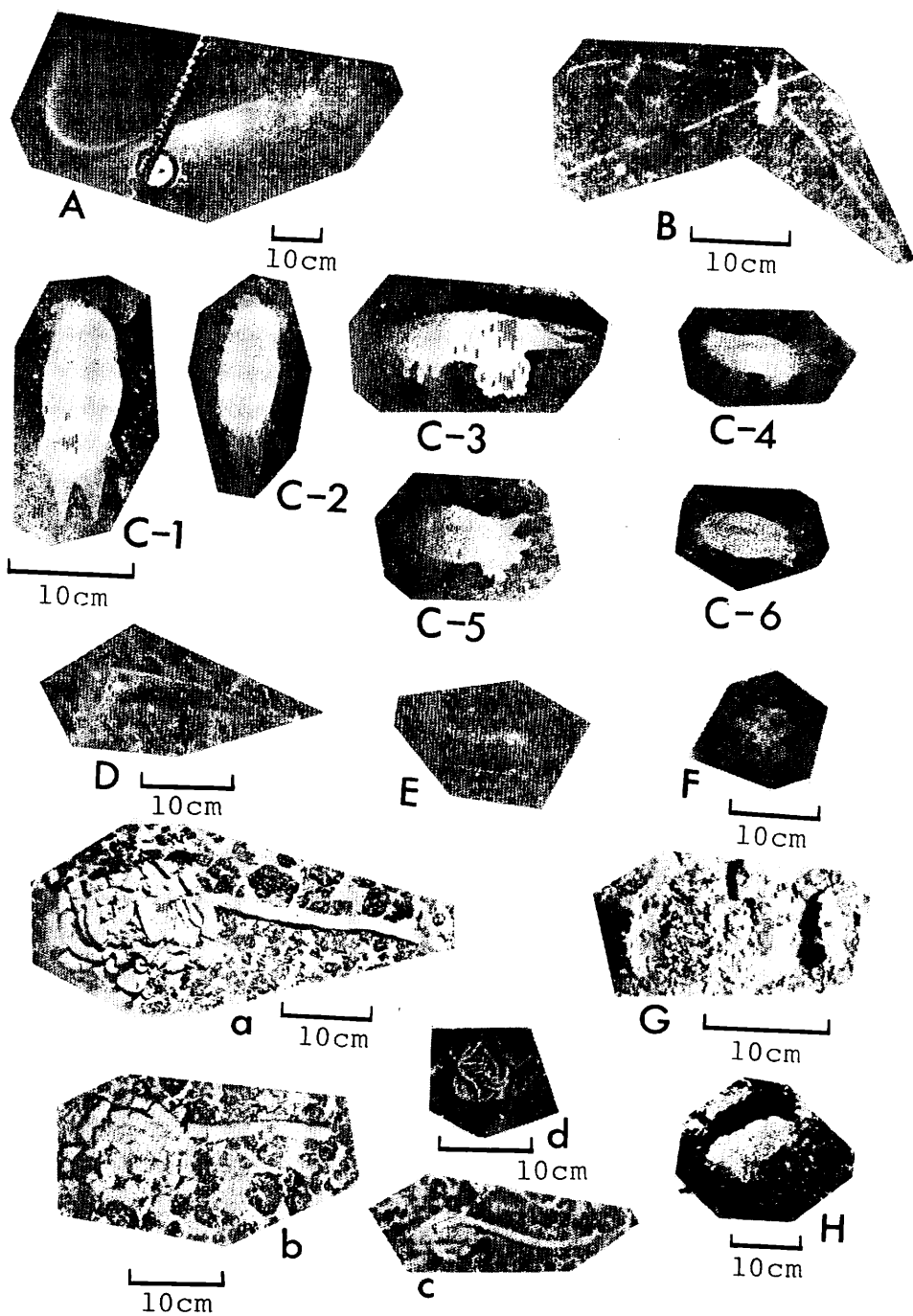
### Benthonic activities

Fig. X-9 and Figs. X-10-12 show the pictures of benthonic organisms and their traces of activities, taken by the deep sea 35 mm camera at St. 1068 (C-13) and St. 1076 (C-14).

In the pictures from St. 1068 (Fig. X-9) there were recognized eight types of organisms (A to H of the figure). A is a type of fish with 80 cm length. B is a sea spider like organism. C-1 to C-6 are a similar type of holothurian (sea cucumber). F is a sponge like organism similar to that recognized at St. 737 (C-12) in GH77-1 cruise. Traces of organism activities are mostly of coprolites and are not usually left on the bottom of high cover ratio area due to the hard surface nature. Coprolites of a, b and c types also were recognized abundantly in high cover ratio areas in GH77-1 and GH76-1 survey areas.

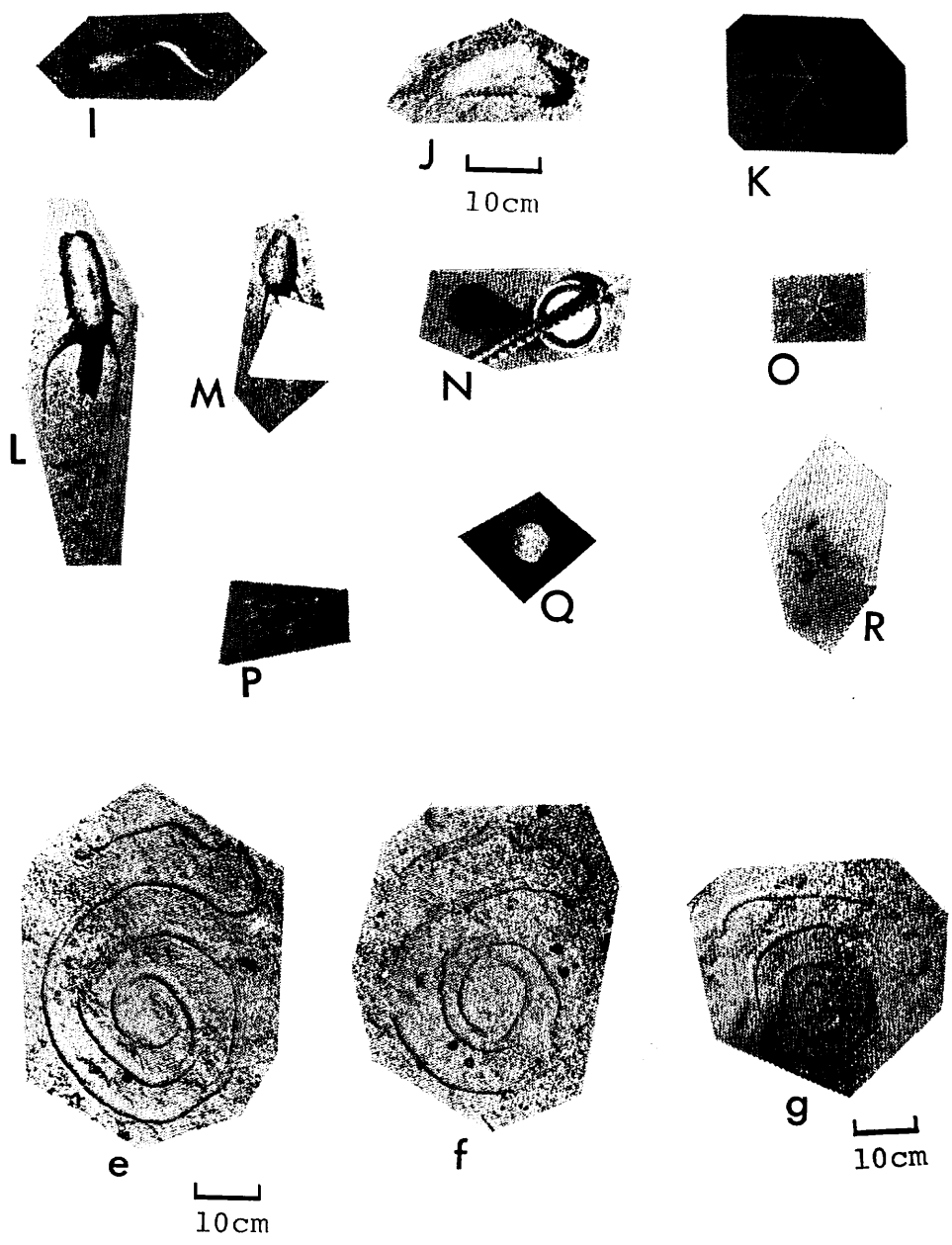
In St. 1076, various types of organisms were recognized (I to R of Fig. X-10). Also, various types of coprolites were recognized (e to r of Figs. X-10 and 11). Among them types of e, f, g, h, i, and j are most abundant. These types of coprolites also were recognized at St. 414A-3 in GH76-1 cruise, and are typically





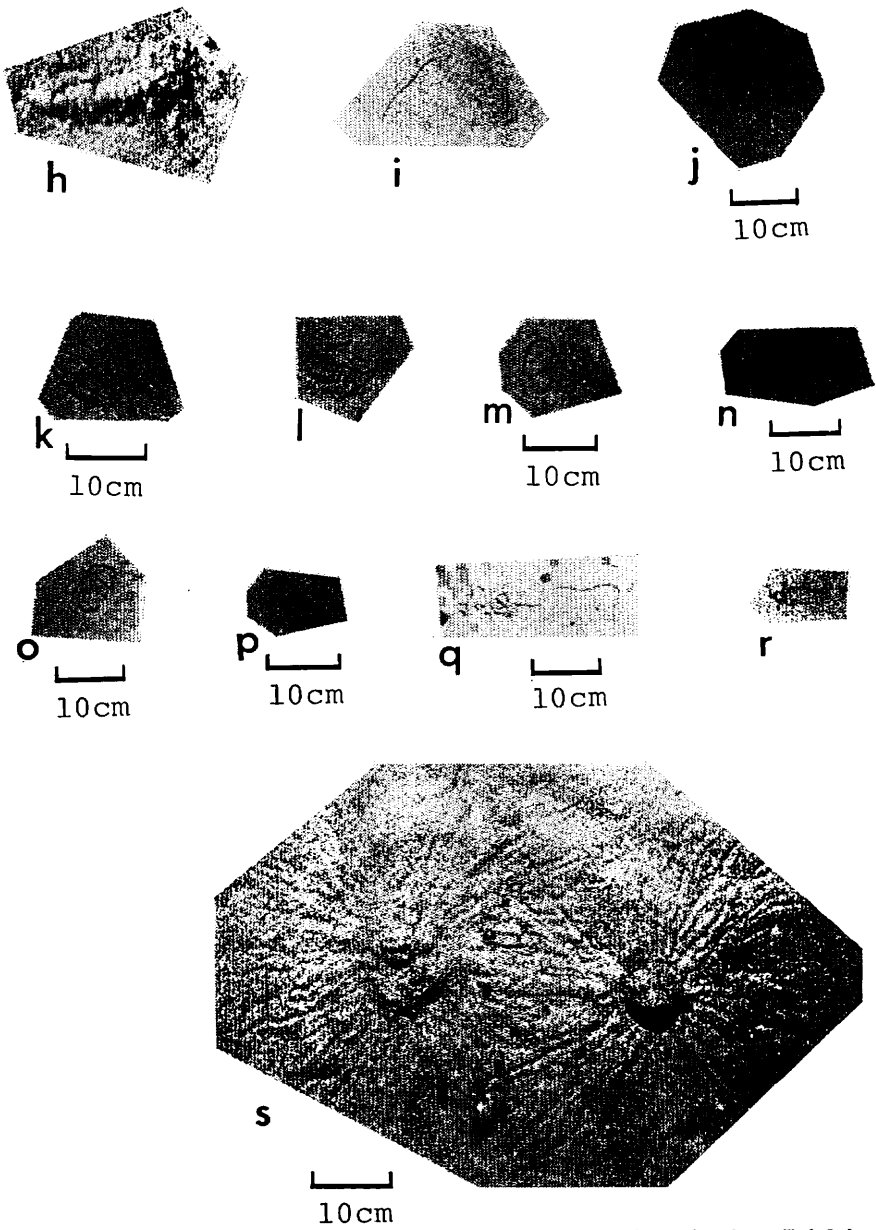
ST. 1068 C-13 5443m-5448m

Fig. X-9 Benthonic organisms (A-H) and coprolites (a-d) at St. 1068.



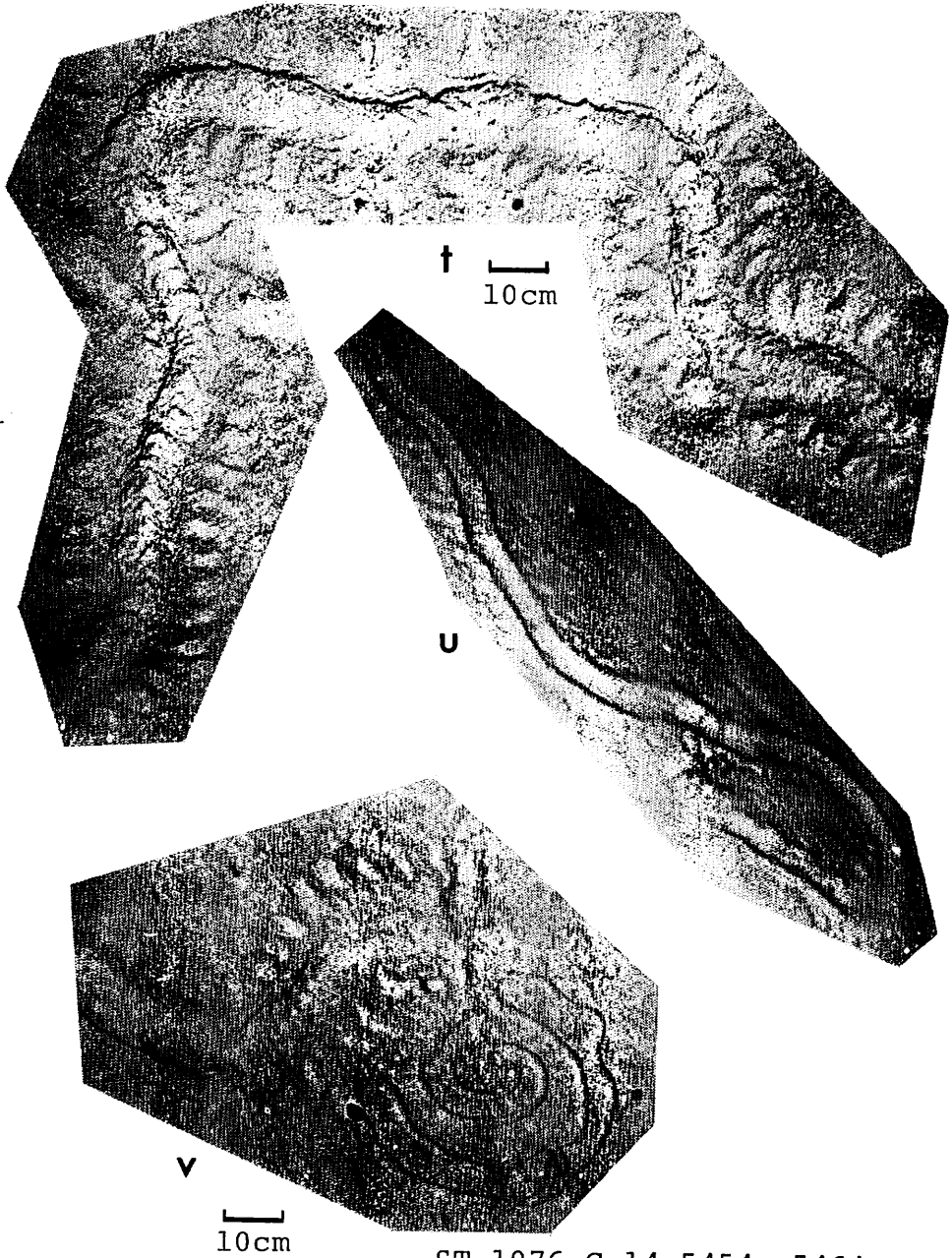
ST.1076 C-14 5454m-5464m

Fig. X-10 Benthonic organisms (I-R) and coprolites (e-g) at St. 1076.



ST.1076 C-14 5454m-5464m

Fig. X-11 Coprolites (h-r) and a trace (s) at St. 1076.



ST. 1076 .C-14 5454m-5464m

Fig. X-12 Traces of grooved form at St. 1076.

seen in the area with less nodule distribution. Some trails forming grooves with about 10 cm wide and a few meters length were recognized (t, u, v of Fig. X-12).

### References

- KINOSHITA, Y. (1977) Manganese nodules and benthonic activities by deep sea photography. In A. MIZUNO and T. MORITANI (*eds.*), *Geol. Surv. Japan Cruise Rept.*, no. 8, p. 78-93.
- , MORITANI, T. and HANDA, K. (1979) Manganese nodule occurrence and benthonic activities observed from deep sea photographs. In T. MORITANI (*ed.*), *Geol. Surv. Japan Cruise Rept.*, no. 12, p. 106-130.